Development of a simple mathematical model and an optimization method for gas lift experimental studies

Asli Karacelik[a,*], Christian Holden[a]

[a]*Department of Mechanical and Industrial Engineering, Norwegian University of Science and Technology, Trondheim, 7491, Norway*

Abstract

Gas lift systems, also known as gas lift or airlift pumps, offer versatile application areas, such as enhancing production efficiency, initiating well production, and well unloading. Therefore, various industries use these simple systems to improve production, including oil and gas, deep-sea mining, aquaculture, wastewater treatment, biotechnology, and nuclear energy. This paper provides a deeper understanding of gas lift systems through a simple and dynamic mathematical model with an explicit formulation. The model contains correlation functions that describe the relationship between volumetric gas and liquid flow rates. The unique approach employed by the proposed model to determine the multiphase flow rate has the potential to open new avenues for research. We compare the model with the previous five different laboratory studies to validate it. The proposed mathematical model is limited to a two-phase flow regime and laboratory scale studies and is free of tuning parameters and measurements. This study presents three main arguments. First, the insights given by the model facilitate an accurate interpretation of the laboratory results. Second, changing our perspective allows us to more easily and quickly identify optimal points. Third, we reveal that the optimal gas inflow rate becomes zero above a certain reservoir pressure.

Keywords: airlift, gas lift pump, experiment, mathematical model, multiphase flow

Nomenclature

α	Volume fraction
$\bar{\alpha}$	Average volume fraction
$\bar{\rho}$	Average density
$\bar{p}$	Average pipe pressure
ρ	Density
Ξ	Ratio of the superficial velocities
A	Pipe area
D	Pipe diameter
g	Standard acceleration of gravity
H	Pipe height
M	Molar mass
m	Mass
p	Pressure
p_h	Hydrostatic pressure
p_{atm}	Standard atmospheric pressure
Q	Volumetric flow rate
R	Molar gas density
S	Submergence ratio
T	Temperature
U	Superficial velocity
V	Pipe volume
w	Mass flow rate

Subscripts

0	Initial value
bot	Bottom of the pipe
g	Gas
in	Pipe inlet
inj	Injection
l	Liquid
mix	Mixture of fluids
out	Pipe outlet
res	Reservoir
top	Top of the pipe

*Corresponding author.

Email addresses: asli.karacelik@ntnu.no (Asli Karacelik), christian.holden@ntnu.no (Christian Holden)

1. Introduction

Gas lift systems counteract the effect of decreasing reservoir pressure over time. Injected gas reduces the fluid density, leading to higher production rates. In other words, they act as pumps; hence, the system is also known as gas lift pumps. Besides increasing production rates, continuous and intermittent gas lift systems [1, 2, 3] initiate well production, and continuous systems attenuate slugging. However, the gas lift effect reverses during phase inversion in oil-water flows, and the production rate decreases [4, 5, 6].

Slugging occurs towards the end of the reservoir life when the reservoir pressure is insufficient to carry the fluid to the surface. If the reservoir pressure declines to a level that causes the flow to cease entirely, a gas lift system can reinitiate the flow. In flow initiation, slugging arises due to low gas inflow rate [7]. There are two types of slugging: hydrodynamic and severe slugging. High-frequency slugging and continuous flow define hydrodynamic slugging, while low-frequency and intermittent flow characterize severe slugging. Severe slugging is classified based on several factors: slug length, maximum pressure, pressure fluctuation, liquid fallback, and blockage [8]. Researchers have developed numerous mathematical models to describe the behavior of slugging in pipeline/riser systems [9, 10, 11, 12, 13].

Various studies proposed hybrid methods—combining passive and active approaches—to prevent slugging. Passive methods, such as flow conditioners, do not require energy. One example of a hybrid method is merging mixers and gas lift systems [14]. Brasjen et al. (2014) [14] reported a high efficiency in mitigating slugging compared to non-hybrid models.

Jansen and Shoham (1994) [15] suggested combining gas lift and choking techniques to mitigate slugging while reducing production costs. The choking method regulates pressure in the flowline by adjusting the choke valve opening. Empirical investigations have revealed that the gas lift technique alone necessitates substantial gas injection to stabilize the system [12, 16]. However, excessive gas injection may increase the total pressure in the system. Although Jansen and Shoham (1994) claimed that the gas lift method is advantageous because it decreases the hydrostatic pressure, it remains ambiguous whether there is an increase in production rate in their study (refer to Fig. 6 and 11 in [15]).

Some researchers [17, 18, 19, 20, 21] have stated that frictional forces dominate at high gas injection rates, so the production rate declines. While frictional forces increase with gas velocity, the static and dynamic pressure of the gas also increases. Therefore, it is imperative to consider both the frictional forces and the resulting pressure changes when analyzing the effects of high gas injection rates on the production rate. Additionally, Guet and Ooms (2006) [22] have reported that frictional losses account for less than 10% of the total pressure for low to moderate liquid flow rates, and the gravitational pressure term is dominant in gas lift applications.

Moreover, gas injection reduces hydrostatic pressure, increasing the liquid outflow rate. However, the injected gas concurrently occupies space within the pipe, displacing the liquid. Consequently, further gas injection fails to raise the liquid outflow rate. In addition, suppose the pressure of the injected gas surpasses that of the bottom hole pressure, which is the pressure at the bottom of the riser. In that case, the gas injection increases the static pressure (gas mass) within the pipe, resulting in a more rapid decline in the liquid outflow rate after reaching its maximum value.

Two studies have examined the effect of gas injection angles on the production rate. The traditional method involves injecting gas downwards. However, recent research by Rodrigues et al. (2021) [23] discovered that injecting gas at orthogonal or upward angles decreases pressure drop in the riser. However, downward injection remains advantageous for low gas flow rates. In contrast, Guerra et al. (2022) [24] found that the impact of upward and downward injections is almost indistinguishable. The finding in [24] may be due to using a volumetric pump to transport water. Volumetric pumps are positive displacement pumps providing the same quantity for each cycle. Here, it is noteworthy that the purpose of a gas lift is to increase production, and this type of pump cannot achieve this. [1]

Casing heading instability (Fig. 1) is another issue in gas lift systems [25]. The instability cycle commences when gas starts flowing through the casing into the tubing. As a result, the fluid density within the tubing decreases, increasing the pressure difference between the tubing and casing. The increase in pressure difference results in a sudden and excessive inflow of gas into the tubing; the casing pressure drops significantly, making it insufficient to overcome the hydrostatic pressure in the tubing, thereby preventing the gas passage from the casing to the tubing. Therefore, gas starts to accumulate in the casing. When the pressure is sufficient to lift the fluid in the tubing, the gas flows again from the casing to the tubing, and a new cycle begins.

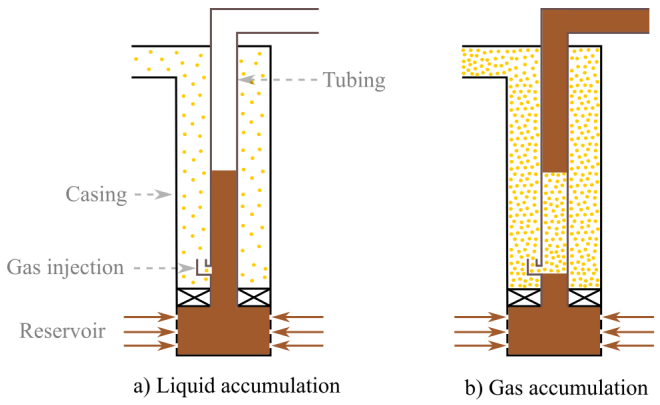

Figure 1: Casing heading instability in gas lift systems.

Aamo et al. (2005) [26] investigated the stabilization of casing heading instability using topside measurements in a single gas lift system with a nonlinear observer. Differently, Eikrem et al. (2006) [25] studied the casing heading instability of dual gas

[1] They also used the term "cumulative density function" instead of "probability density function".

lift wells, which combines two production zones in one production casing. Later, Eikrem et al. (2008) [27] suggested several simple automatic control strategies for a single gas lift well. Lastly, Larsen and Asheim (2014) [17] applied frequency control at the gas injection inlet and the production choke valve to obviate casing heading instability.

Gas lift systems improve the cooling performance of accelerator-driven subcritical nuclear reactors [28, 29]. These reactors have gained attention due to their safety [30] and capability to convert long-lived radioactive waste into short-lived waste [31]. The other experimental gas lift studies include liquid-assisted gas-lift unloading [32] and a comparative analysis of plunger lift and gas lift [33]. Qi et al. (2020) [33] highlighted that the two methods are incomparable because the gas lift is continuous, and the plunger lift is intermittent. Considering this, they evaluated the methods for gas consumption using the same liquid volume.

1.1. Problem statement

In the literature, simple and dynamic gas lift models require severe tuning or parameter measurements to predict the gas lift behavior accurately. As a solution, we propose a more generalized model for laboratory gas lift studies, which can provide insight into system behavior before conducting experiments. This new model and the proposed simple optimization method reduce time-consuming pre-experimental work. Moreover, researchers can employ it for control applications. Lastly, it prevents misleading commentary on results, as the gas lift method may not increase the production rate depending on reservoir pressure.

Since we uncovered the effect of reservoir pressure on the gas lift optimization problem, we have performed a thorough literature review on gas lift laboratory experiments to determine whether researchers consider reservoir pressure when designing their experimental setups. However, we could not find any analysis regarding this issue.

2. Method

The code utilized in this study is accessible through the GitHub webpage[2]. We performed this study with an Intel Core i7-10610U CPU @1.80 GHz @2.30 GHz and a 64-bit Windows operating system.

The suggested model for the air-water system requires only four essential parameters to initiate the code. These parameters include the initial volume fraction, submergence ratio, pipe height, and pipe diameter. The simplicity of the model's input requirements renders it a practical and efficient instrument for analyzing the system's behavior.

Note that the liquid volume fraction in the pipe and the submergence ratio are the same when the pipe diameter is constant. However, the initial volume fraction should be smaller than the submergence ratio to initiate the flow in this study because the algorithm cannot compute scenarios without flow.

[2] https://github.com/asli-karacelik/gaslift-lab-model.git

2.1. Gas lift system

In our laboratory-scale gas lift model, water is the reservoir liquid, and the air is the injected gas, as depicted in Fig. 2. Gas injection is at the bottom of the vertical pipe, equivalent to the pipe's bottom pressure. Other than the density of the injected gas, physical and chemical parameters remain constant and do not change with temperature and pressure. Table 1 shows the values of constants acquired from the National Institute of Standards and Technology (NIST), US Department of Commerce (refer to physical [34] and chemical [35] constants on the NIST website). In section 2.3, we present the calculation of the initial points of the optimization problem.

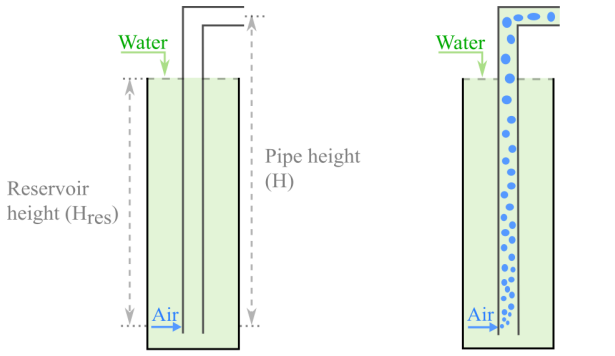

(a) No flow before air injection (b) Flow after air injection

Figure 2: Air lift process diagram.

2.2. Mathematical model of the gas lift system

Eikrem et al. (2004) [36] published a simple and dynamic mathematical model of gas lift for process control studies. The model consists of three states representing mass accumulations. They tuned the model using valve coefficients and did not delve into its physical interpretation.

The authors extended their work in 2006 [25] by introducing two additional states. Understandably, some typographical errors may have occurred because of the publication pressure on the researchers. In particular, they mix up the gas mass in the annulus with the oil mass in the tubing. For example, in the equation below (refer to Eq. (22) in [25]), the specific volume of the oil is multiplied by the gas mass in the tubing to calculate the oil volume in the tubing:

$$p_{wh} = \frac{RT_w}{M} \frac{x_1}{L_w A_w - v_o x_2}, \tag{1}$$

where p_{wh} is the wellhead pressure, R is the molar gas constant, T_w is the temperature in the tubing, and M is the molar mass of the gas. The states, x_1 and x_2 are the gas mass in the annulus and the gas mass in the tubing, respectively. L_w and A_w are the tubing's length and cross-sectional area, and v_o is the specific volume of the oil.

Subsequently, Ribeiro et al. (2016) [18] incorporated frictional forces into the mathematical model proposed by Eikrem et al. (2004) [36]. The study highlighted that friction is necessary for obtaining a gas lift performance curve. That means

Table 1: Constants

Constant	Symbol	Value	Unit
Density of water	ρ_l	0.99821	g/cm^3
Acceleration of gravity	g	980.665	cm/s^2
Discharge coefficient	C_d	$1/\sqrt{2}$	-
Molar gas constant	R	8.314462618×10^7	g·cm^2/(K·mol·s^2)
Molar mass of air	M_g	28.9586	g/mol
Temperature	T	293.15	K

without friction, gas injection would not affect the liquid outflow rate. Instead, the liquid outflow rate would continue to rise. Although the frictional forces contribute to the flow rate decrement, we posit that gas accumulation in the pipeline is the primary cause of this reduction. The density of gas injection, i.e., pressure, determines the degree of gas accumulation. The previous experimental studies on airlift pumps [7, 37, 38, 39, 40, 41] demonstrate that an increase in gas inflow rate does not necessarily lead to a decrease in the liquid outflow rate, which remains almost constant in these studies.

Lastly, Dielh et al. (2017) [42] combine existing models, including the model of Eikrem et al. (2004) [36], to create a general model for slugging. This model characterizes casing heading instability-induced and terrain/riser-induced slugging.

We present a novel zero-dimensional mathematical model featuring two states for laboratory applications. The critical distinction between our model and the approach taken by Eikrem et al. (2004) [36] is that the propounded method does not employ a valve equation to calculate the gas outflow rate. We derived our model through a rigorous focus on the physical principles governing the system without recoursing to measurements or tuning.

The proposed mathematical model assumes linear relationships between the parameters at the top and bottom of the pipe and comprises explicit formulas, as indicated hereunder.

The total volume of the pipe is

$$V = \frac{\pi D^2}{4} H, \tag{2}$$

where D, H, and L denote diameter, height, and length, respectively.

The liquid volume in the pipe is

$$V_l = \frac{m_l}{\rho_l}, \tag{3}$$

where m_l is the liquid mass in the pipe and ρ_l is the density of the liquid.

The average density of the gas in the pipe is

$$\bar{\rho}_g = \frac{m_g}{V - V_l}, \tag{4}$$

where m_g is the gas accumulation.

The average pressure at the pipe is

$$\bar{p} = \frac{\bar{\rho}_g R T}{M_g}, \tag{5}$$

where R is the molar gas constant, T is the average temperature, and M_g is the molar mass of gas.

The average density of the mixture in the pipe is

$$\bar{\rho}_{mix} = \frac{m_g + m_l}{V}. \tag{6}$$

The hydrostatic pressure is

$$p_h = \bar{\rho}_{mix} g H, \tag{7}$$

where g is the standard acceleration of gravity.

The pressure at the top of the pipe is lower than the average pressure in the pipe due to hydrostatic pressure. To account for this difference, we assume that average pressure represents the pressure in the middle of the pipe, which indicates a uniform linear decline in pressure throughout the pipe. Consequently, the pressure at the top of the pipe is given by

$$p_{top} = \bar{p} - \frac{p_h}{2}. \tag{8}$$

The density at the top of the pipe is

$$\rho_{g,top} = \frac{p_{top} M_g}{RT}. \tag{9}$$

The pressure at the bottom of the pipe is

$$p_{bot} = \bar{p} + \frac{p_h}{2}. \tag{10}$$

Here, we ignored head losses. Frictional forces are negligible at low velocities and short distances, while losses stemming from fittings may be significant at low velocities. We introduce losses in the valve equation shown in Eq. (18).

The average liquid volume fraction in the pipe is

$$\bar{\alpha}_l = \frac{V_l}{V}. \tag{11}$$

The average gas volume fraction in the pipe is

$$\bar{\alpha}_g = 1 - \bar{\alpha}_l. \tag{12}$$

Boyle's law states that pressure and volume are inversely proportional when the temperature is constant for a given gas mass within a closed system. This fundamental principle highlights that as the pressure increases, the volume decreases correspondingly, and vice versa. When applying this principle, we assumed that the gas mass distribution is homogeneous within the pipe. Consequently, the gas volume fraction at the top of the pipe given by

$$\alpha_{g,top} = \frac{\bar{\alpha}_g \bar{p}}{p_{top}}. \tag{13}$$

The gas volume fraction at the bottom of the pipe is

$$\alpha_{g,bot} = 2\bar{\alpha}_g - \alpha_{g,top}. \tag{14}$$

The reservoir height shown in Fig. 2 is

$$H_{res} = HS, \tag{15}$$

where S is the submergence ratio.

The reservoir pressure is

$$p_{res} = p_{atm} + \rho_l g H_{res}. \tag{16}$$

Bernoulli's principle states the relationship between pressure and energy (kinetic and potential) along a fluid's streamline. This principle applies to inviscid and incompressible fluids in a steady-state flow. It forms the basis for quantifying the flow of incompressible fluids without factoring in energy dissipation. The mass flow rate through a restriction—derived from Bernoulli's principle and the continuity equation—is given by

$$w = C_d A \sqrt{2\rho\Delta p}, \tag{17}$$

where w is the mass flow rate, A is the cross-sectional area of the orifice, ρ is the density of the fluid, Δp is the pressure difference across the orifice, and C_d is the discharge coefficient, accounting for the energy losses. C_d is 1 for ideal fluids, i.e., inviscid and incompressible fluids. However, when considering energy losses, C_d decreases to 0.60-0.65 for orifices with sharp edges and is about 0.8-0.9 for rounded edges [43].

The next step is determining the discharge coefficient for the experimental studies [7, 38, 44, 45, 46] employed in this research. Owing to the simplicity and comparability of their experimental setups, we propose the following equation for the liquid inflow rate:

$$w_{l,in} = (1 - \alpha_{g,bot}) C_d A \sqrt{2\rho_l \max(0,\ p_{res} - p_{bot})}, \tag{18}$$

where p_{res} is the reservoir pressure and A is the cross-sectional area of the pipe. Assuming that the gas and liquid come from the same pipe, it is sensible to scale Eq. (17) with the area fraction. The volume fraction can supplant the area fraction for the same height as shown in Eq. (18). In this equation, C_d is $1/\sqrt{2}$ (approximately 0.7), which differs from the abovementioned values. The discrepancy arises from the fluid inlet design, which varies compared to those with sharp and rounded edges Fig. 2. We anticipated that the head losses in our system would be lower than those associated with sharp edges but higher than those with rounded edges. As a result, we chose a discharge coefficient that falls between sharp and rounded edges.

Determining the flow rate of multiphase flows poses more challenges, as Bernoulli's equation cannot correctly estimate multiphase flow rates. Modified versions of Bernoulli's equation [47] exist for compressible flows, but we need a different approach for multiphase flows. For instance, Eikrem et al. (2004) [36] substantially adjusted the valve equation with valve coefficient to match their theoretical and experimental results. The valve equation is similar to Eq. (17); the only difference is that the valve coefficient replaces the discharge coefficient. After calculating the total outflow rate, Eikrem et al. (2004) [36] determine the flow rates of individual phases by multiplying the total outflow rate with corresponding mass fractions.

The outflow is a mixture of liquid and gas phases; we treat them separately to calculate individual outflow rates. The equation utilized for the liquid inflow rate also determines the liquid outflow rate. Consequently, the liquid outflow rate is

$$w_{l,out} = (1 - \alpha_{g,top}) C_d A \sqrt{2\rho_l \max(0,\ p_{top} - p_{atm})}, \tag{19}$$

where p_{atm} is the standard atmospheric pressure.

We propose a new method for calculating the gas outflow rate. The first step entails computing the volumetric liquid outflow rate using the following equation:

$$Q_{l,out} = \frac{w_{l,out}}{\rho_l}. \tag{20}$$

A volumetric flow rate represents fluids' velocity for the same cross-sectional area. However, the velocity difference in gas and liquid phases varies significantly depending on the flow pattern, such as slug, churn, annular, etc. Understanding the behavior of gas and liquid in a container is essential to understanding their velocity differences. Imagine a vertical pipe containing liquid and another pipe containing gas. The conditions are the same for both the gas and the liquid phases. The liquid half-fills the pipe and remains stationary, while the gas expands and fills the pipe. This scenario illustrates that gas velocity is higher than liquid velocity under the same conditions, as the density of gasses is lower than that of liquids.

Given the above phenomena, we can correlate volumetric gas and liquid flow rates. If the other phase were also liquid, we could easily calculate the volumetric liquid flow rates using volume fractions. However, since the liquid is incompressible and the gas is compressible, we must consider the effect of compressibility on the volumetric gas flow rate. If the liquid were gas, it would occupy the pipe entirely, and we assume this occupation is instantaneous. To account for the incompressibility of the liquid phase, we divide the liquid volumetric flow rate by the liquid volume fraction. Once we compensate for the incompressibility factor, we can treat gas and liquid as the same phase and use the volume fractions to calculate the volumetric gas outflow rate. Based on this rationale, we propose a correlation function for the volumetric gas outflow rate:

$$Q_{g,out} = \frac{Q_{l,out}}{\alpha_{l,top}} \frac{\alpha_{g,top}}{\alpha_{l,top}}. \tag{21}$$

As a supplementary note, dividing Eq. (21) with the pipe's cross-sectional area gives the correlation for superficial gas velocities:

$$\Xi = \frac{U_g}{U_l} = \frac{1}{\alpha_l}\frac{\alpha_g}{\alpha_l}, \tag{22}$$

where U_g is the superficial gas velocity, and U_l is the superficial liquid velocity.

The gas mass outflow rate is

$$w_{g,out} = Q_{g,out}\rho_{g,top}. \tag{23}$$

In practical applications, the pressure of gas injection is usually slightly higher than the bottom hole pressure to ensure maximum efficiency [48]. The reviewed laboratory studies on airlift pumps prefer the pressure at the bottom of the pipe, bottom hole pressure, as the injection pressure. For comparison with other studies, the density of the lift gas at the inlet conditions is given by

$$\rho_{g,inj} = \frac{p_{bot}M_g}{RT}. \tag{24}$$

The gas mass inflow rate is

$$w_{g,inj} = Q_{g,inj}\rho_{g,inj}, \tag{25}$$

where $Q_{g,inj}$ is the volumetric inflow rate of the injected gas.

The gas mass accumulation is

$$\dot{m}_g = w_{g,inj} - w_{g,out}. \tag{26}$$

The liquid mass accumulation is

$$\dot{m}_l = w_{l,in} - w_{l,out}. \tag{27}$$

2.3. Optimization

The volumetric gas inflow rate is the input, while liquid and gas masses represent the states in the proposed dynamic model. The output of this model is the liquid outflow rate. Notably, the gas inflow rate is independent of the initial estimates of the states because of the stabilizing effect of gas flow on these states. As a result, MATLAB's fsolve function can provide a steady-state solution for specified volumetric gas inflow rates.

The optimization algorithm is the trust-region-dogleg algorithm, the default algorithm in fsolve. We obtain the corresponding steady states by incorporating gas inflow rates into this algorithm using a for loop. Ultimately, this approach identifies the maximum liquid outflow rate within a predefined range of gas inflow rates.

By considering the physical implications of the system, we can determine the optimal input without resorting to intricate optimization algorithms. The initial estimates for the liquid and gas mass in the pipe are given by

$$m_{l,0} = V\alpha_{l,0}\rho_l, \tag{28a}$$

$$m_{g,0} = \frac{p_{top}V(1-\alpha_{l,0})M_g}{RT}, \tag{28b}$$

where $\alpha_{l,0}$ is the initial liquid volume fraction. While the initial guesses do not affect the optimization problem, they must be within the physical domain to avoid errors. Hence, ensuring the initial guesses are physically plausible is an essential prerequisite for the optimization procedure. Therefore, we determine the initial gas and liquid mass from the initial liquid volume fraction, which is straightforward to visualize and implement.

Scaling is another crucial practice to secure a smooth optimization procedure. Rather than non-dimensionalizing and scaling the nonlinear model, we leveraged the centimeter–gram–second system of units (CGS). This choice is because scaling nonlinear models may not accurately replicate their nonlinear behavior.

When scaling is not a viable solution, an alternative approach would be implementing tighter tolerances, which require higher processing time. In the trust-region-dogleg algorithm, optimality tolerance is absolute, while function and step tolerance are relative. Iterations terminate under the following conditions:

$$\nabla f(x_i) < \text{Optimality Tolerance}, \tag{29a}$$

$$x_i - x_{i+1} < (\text{Step Tolerance})(1 + x_i), \tag{29b}$$

$$|f(x_i) - f(x_{i+1})| < (\text{Function Tolerance})(1 + |f(x_i)|), \tag{29c}$$

where x is the state value.

3. Results and discussion

This study aims to enhance our understanding of gas lift systems while proposing a practical approach to estimate the system's behavior in advance. It is of utmost importance to determine the study range beforehand to observe the effect of the gas lift system. The system's response to gas injection varies depending on the reservoir pressure and whether the study range is above or below the optimal point. Gas injection is redundant if the reservoir pressure is above a certain point or the study range is above the optimal point. On the contrary, when the study range is below the optimal point, the maximum gas flow rate is the optimal point.

3.1. Validation of the mathematical model

We compared our mathematical model to experimental data obtained from previous studies: Stenning and Martin (1968) [44], Kassab et al. (2009) [7], Goharzadeh and Fernandes (2014) [38], Todoroki et al. (1973) [45], and Becaria et al. (2006) [46]. The PlotDigitizer version 3.1.5 extracts the experimental data from these studies. Unlike Goharzadeh and Fernandes (2014) [38], the other studies fitted their experimental data to a function. Therefore, we fitted a seventh-degree polynomial function to the experimental data of Goharzadeh and Fernandes (2014) [38] and extracted the data from this function. The function has a coefficient of determination (R^2) of 0.9974.

The investigated articles employed the volumetric flow rate for gas injection except for Kassab et al. (2009) [7] implementing the mass flow rate. The injection pressure is the average pump pressure in the reviewed articles. Exceptionally, the injection pressure for each trial in Goharzadeh and Fernandes (2014) [38] is close to atmospheric pressure. Thus, we applied atmospheric pressure as the gas injection pressure for the study

of Goharzadeh and Fernandes (2014) [38]. Additionally, Becaria et al. (2006) [46] gradually increased the injection pressure during the experiment.

The proposed mathematical model exhibits a strong correlation with the experimental results obtained by Stenning and Martin (1968) [44], as shown in Fig. 3. However, the experimental findings of Kassab et al. (2009) [7] at low submergence ratios do not align well with our model (Fig. 5). Notably, the difference between theoretical and experimental results is significantly high at submergence ratios of 0.2 and 0.4. For instance, the maximum liquid outflow rate at the submergence ratio of 0.4 is around 147 g/s in the experiment and 205 g/s in theory. However, the maximum liquid outflow rates become substantially close at the submergence ratio of 0.484, approximately 270 g/s in the experiment and 274 g/s in theory. Therefore, we may attribute this difference to experimental errors at the submergence ratio of 0.4 because the variation in liquid outflow rates should not differ significantly between submergence ratios of 0.4-0.484. A similar reasoning also applies to the submergence ratios of 0.2-0.227. Nonetheless, the model fit well at submergence ratios between 0.484-0.750, shown in Fig. 5.

Kassab et al. (2009) [7] identified five flow patterns in their study. The patterns corresponding to low to high gas injection rates are bubbly, bubbly-slug, slug, slug-churn, and annular. After the liquid outflow rate reaches its highest value, the pattern becomes slug-churn, followed by annular flow. In annular flow, gas flow concentrates in the middle and pushes the liquid towards the pipe surface; it renders gas and liquid flow without mixing. This definition explains why the change in gas mass, i.e., pressure, within the pipe is comparatively lower in annular flow than in other flow patterns.

Previous studies [18, 25, 36] utilized average gas pressure as the pipe's top pressure and the mass fractions to determine the fluid outflow rates. However, these calculations lead to significant deviations from experimental results if not adjusted, as demonstrated in Fig. 4. To show this difference, we implement the method of the studies mentioned above without the valve coefficient and compare it with the experimental data of Stenning and Martin (1968) [44] (Fig. 4). The method of the previous studies given by

$$p_{top} = \frac{\rho_g RT}{M_g}, \tag{30a}$$

$$w_{tot,out} = C_d A \sqrt{2\rho_{mix} \max(0,\ p_{top} - p_{atm})}, \tag{30b}$$

$$x_l = \frac{m_l}{m_l + m_g}, \tag{30c}$$

$$w_{l,out} = x_l w_{tot,out}, \tag{30d}$$

$$w_{g,out} = w_{tot,out} - w_{l,out}. \tag{30e}$$

The pipe volume is relatively small in the study of Goharzadeh and Fernandes (2014) [38], approximately ten times smaller than Stenning and Martin (1968) [44]. However, the range of gas injection rates is the same in both studies. Our study found that Eq. (21) is ineffective in accurately predicting the liquid flow rates experimentally reported by Goharzadeh and Fernandes (2014) [38] at high gas injection rates (Fig. 6). Specifically, the theoretical model overestimates the gas mass within the pipe, resulting in lower liquid outflow rates than experimentally observed. This discrepancy may stem from the abrupt transition between flow patterns prompted by high gas injection rates as Goharzadeh and Fernandes (2014) [38] reported three different flow regimes: slug, churn, and annular. In contrast, Kasab et al. (2009) [7] observed five flow patterns. The liquid outflow rate may not exhibit a discernible decline after reaching its peak because it reaches the annular flow regime more quickly. Therefore, the gas outflow rate should increase to correspond to this fast flow regime change. Dividing Eq. (21) with liquid volume fraction increases the volumetric gas outflow rate by considering the flow pattern change. In other words, the higher the liquid volume fraction, the lower the gas outflow rate. Therefore, we propose another correlation given by (Fig. 6)

$$Q_{g,out} = \frac{Q_{l,out}}{\alpha_{l,top}^2} \frac{\alpha_{g,top}}{\alpha_{l,top}}. \tag{31}$$

The correlation between the superficial gas and liquid velocities becomes

$$\Xi = \frac{U_g}{U_l} = \frac{1}{\alpha_l^2} \frac{\alpha_g}{\alpha_l}. \tag{32}$$

The experimental findings reported by Todoroki et al. (1973) [45] agree with the predictions derived from our theoretical model. However, the studies above demonstrate a superior fit with the experimental data. The reason is likely to be the higher pipe height used in this study. The pressure difference between the pipe's top and bottom is higher due to increased hydrostatic pressure, affecting the distribution of the gas volume fraction in the pipe. The linear parameter assumptions between the pipe's top and bottom are suboptimal for nonhomogenous gas-liquid mixtures, especially in high pipe heights. Therefore, the suggested correlation for the superficial velocities requires revising for high-riser systems.

Another potential reason for the experiment and theory mismatch may be the higher pressure losses, as Todoroki et al. (1973) [45] employed a suction pipe to transfer liquid from the reservoir to the pipe, unlike other studies that had a direct connection between the reservoir and the pipe.

The substantial difference between our theoretical model and the experimental findings of Becaria et al. (2006) [46] (Fig. 8) necessitated an in-depth examination of the solution quality. Exit flags (Fig. 9) elucidate the reasons explained in Table 2 for the termination of the fsolve algorithm. Moreover, metrics such as the Jacobian condition number and the first-order optimality measure offer critical information for assessing a solution's quality. The ratio of a matrix's largest singular value to its smallest singular value determines its condition number, while the first-order optimality measure in Fig. 9 indicates the maximum absolute value (infinity norm) of $\nabla f(x)$, defined as follows:

$$\text{first order optimality measure} = \|\nabla f(x)\|_\infty, \tag{33}$$

where x signifies states—gas and liquid mass within the pipe.

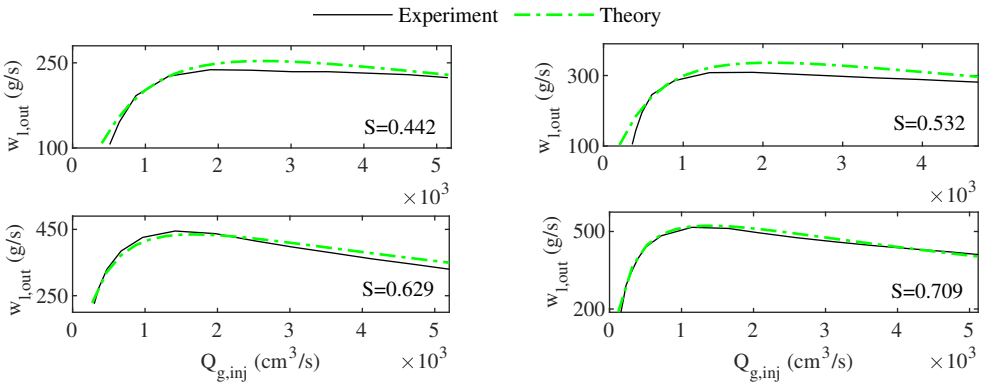

Figure 3: Comparing the mathematical model with experimental data from Stenning and Martin (1968) [44]. S is the submergence ratio. The pipe diameter and height are 2.54 cm and 426.72 cm, respectively.

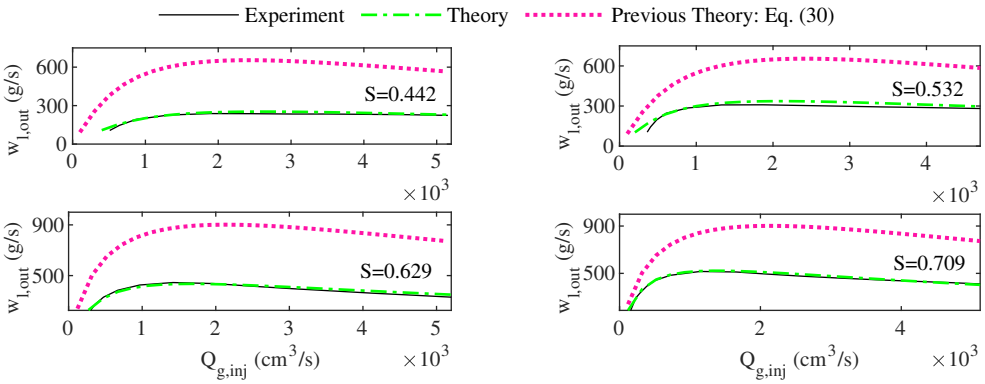

Figure 4: The proposed mathematical model and the modified model shown in Eq. (30) compared with the experimental study of Stenning and Martin (1968) [44]. The previous model Eq. (30) employs mass fractions to compute the gas and liquid outflow rates. S is the submergence ratio. The pipe diameter and height are 2.54 cm and 426.72 cm, respectively.

Table 2: Explanation of the exit flags in fsolve

Exit flag	Explanation
-2	No solution exists.
-1	The algorithm terminated due to a plot or output function.
0	The number of specified iterations is insufficient.
1	A solution exists with minimal first-order optimality.
2	A solution exists when the Jacobian is undefined at x or when the specified tolerance exceeds the change in x.
3	A solution exists when the specified tolerance exceeds the change in residual

x indicates states.

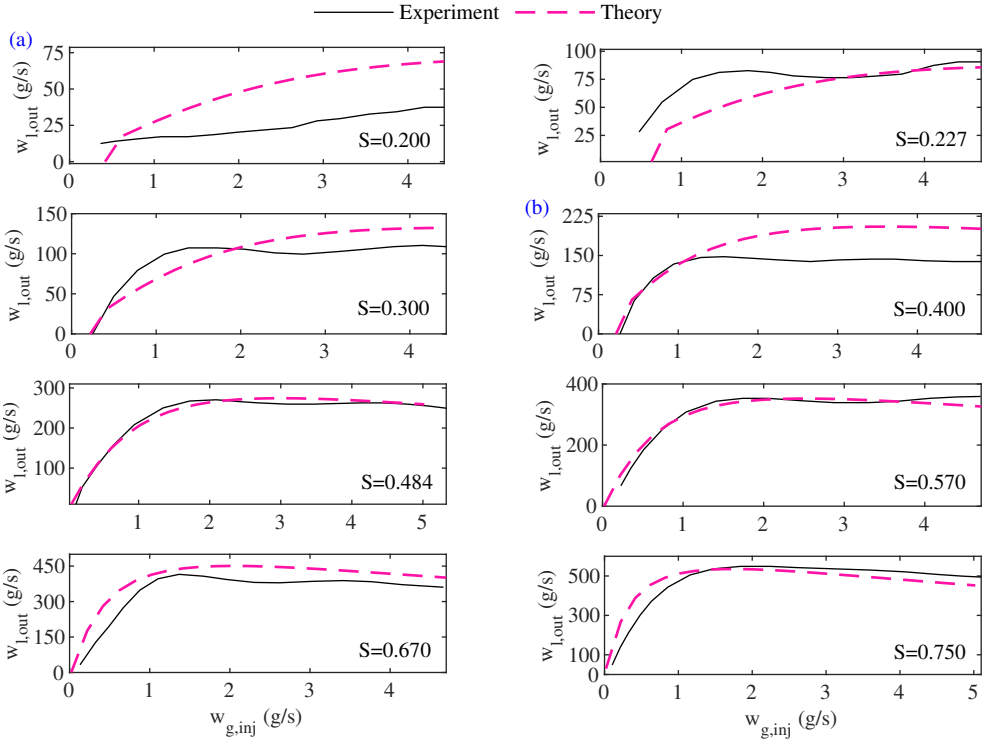

Figure 5: Comparing the mathematical model with experimental data from Kassab et al. (2009) [7]. S is the submergence ratio. The pipe diameter and height are 2.54 cm and 375 cm, respectively. In (a) and (b), we attribute the differences between theory and experiment to experimental errors explained in the text.

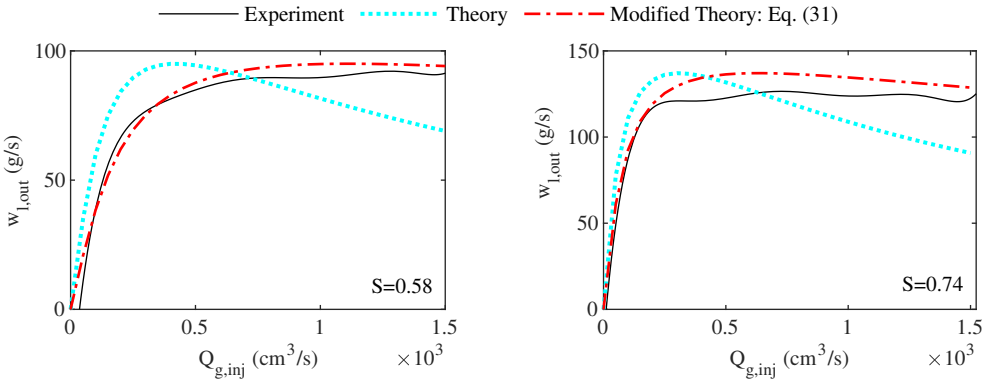

Figure 6: The proposed mathematical model and the modified model shown in Eq. (31) compared with experimental data from Goharzadeh and Fernandes (2014) [38]. S is the submergence ratio. The pipe diameter and height are 1.9 cm and 80 cm, respectively.

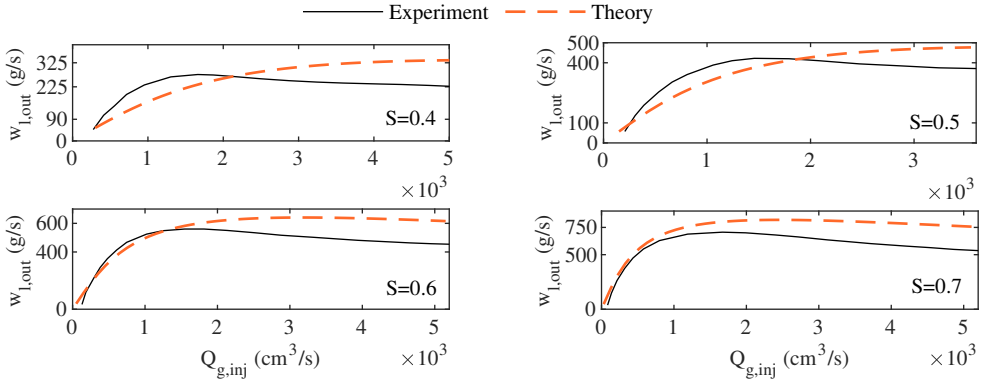

Figure 7: Comparing the mathematical model with experimental data from Todoroki et al. (1973) [45]. S is the submergence ratio. The pipe diameter and height are 2.83 cm and 750 cm, respectively.

The algorithm cannot solve the problem at low gas injection rates because it relies on the steady-state solution. Although there is liquid inflow, there is no liquid outflow at low gas injection rates. The gas inflow is insufficient to lift the liquid to the top of the pipe, rendering the problem unsolvable by the algorithm. However, it accurately resolves the problem with a Jacobian condition number of 4-5$\times 10^5$ when there is a liquid outflow. Hence, the issue at hand is not numerical.

Becaria et al. (2006) [46] compared small-diameter production tubings with conventional ones to determine the role of the pipe diameter in low reservoir pressure. Their results indicated a higher liquid outflow rate in smaller-diameter pipes, a phenomenon attributed to the effects of adhesive and cohesive forces. Becaria et al. addressed these effects by incorporating the liquid film fallback in their mathematical model, accounting for the impact of viscous drag forces and surface tension on the thickness of the downward-flowing film. They examined pipes with diameters of 0.4 cm, 0.8 cm, and 1.2 cm to determine liquid outflow rates. We compared our mathematical model against the experimental results for the 1.2 cm diameter pipe [46]. Our findings may support the same argument as Becaria et al. regarding the effects of adhesive and cohesive forces on liquid outflow rate in small-diameter pipes.

3.2. Effect of reservoir pressure on the optimization problem

The literature shows three reservoir types that imitate reservoir pressure: hydrostatic pressure, pumps, and a constant-pressure tank. While pumps are the preferred choice among most oil and gas researchers, they might not accurately mimic a reservoir's behavior because the liquid outflow rate depends on the pump curve. Specifically, the pressure difference between the pump inlet and outlet can alter the liquid outflow rate under gas lift, meaning the liquid outflow rate would be higher without the pressure difference. Therefore, we must know how this pressure difference affects the liquid outflow rate in gas lift experiments.

Although hydrostatic pressure is a viable option, researchers must be careful to maintain it during the experiments. Employing hydrostatic pressure eliminates the need to assess the suitability of reservoir pressure for a gas lift experiment. Since hydrostatic pressure is inherently low, it can provide higher liquid outflow rates with gas lift.

A constant pressure tank seems to be an appropriate option. However, this option is more challenging to apply than the others, so only one article [33] implemented the constant water pressure tank in their study.

The industry utilizes gas lift systems when the production rate decreases due to low reservoir pressure. Consequently, researchers must also use gas lift systems in laboratory studies when the reservoir pressure is sufficiently low. However, the problem is how low the pressure should be for specific heights. Our research has revealed reservoir pressure's direct impact on gas lift behavior.

Gas injection lowers hydrostatic pressure in the pipe and increases the pressure at the top. Therefore, there is a delicate balance between reducing the hydrostatic pressure and increasing the top pressure by introducing gas into the system. Eq. (10) for the pressure at the bottom of the pipe specifies this balance. An equal amount of change in the hydrostatic pressure and the top pressure will not increase the liquid outflow rate because they cancel out each other's effect; hence, the pressure at the bottom of the pipe does not change. Therefore, there is a critical pressure beyond which lift gas does not increase the liquid outflow rate. The main reason is that the reservoir pressure becomes sufficiently high to overcome the hydrostatic pressure, which means lift gas is not required.

Fig. 10 shows the reservoir pressure effect on liquid outflow rate during gas lift. At a reservoir pressure of 1.6 atm, we observe a discernible increase in the liquid outflow rate. Conversely, at reservoir pressures of 1.7 atm, a decrease in the liquid outflow rate is evident. Because of low gas injection rates, the solution has numerical issues. However, the observable trend of increase and decrease in the liquid outflow rate is still apparent in the figure.

Additionally, we have created a three-dimensional surface graph (Fig. 11) to show how the reservoir pressure against gas injection affects the liquid outflow rate. The purpose of this graph is to identify the critical reservoir pressure. The color indicators on the graph move towards the right when the pressure is low and become flat for average pressures. However, when the pressure is high, the indicators move slightly towards the left, as depicted in Fig. 11. The pressure and gas injection increments are 0.3 bar and 10 cm^3, respectively. Therefore, the critical pressure is around 1.63 atm, which is a rough estimate, as the pressure and gas increments are not low enough to give a more accurate result.

We present a quantitative comparison of the theoretical and experimental studies in Table 3.2.

4. Conclusion

Gas lift systems increase production rates by decreasing fluid density. Owing to the simplicity and effectiveness of these systems, they have broad application areas from the oil and gas industry to aquaculture. This study aims to provide initial information for planned experiments, save time on preliminary laboratory studies, and prevent misinterpretation of the results. First, we developed a simple and dynamic mathematical model that doesn't require measurements or adjustments. The model includes innovative interpretations of the relationship between volumetric gas and liquid outflow rates that researchers can apply to control systems. Second, we validated the proposed mathematical model with the experimental data from the previous five laboratory studies conducted by different researchers. The results have shown that the proposed model is sufficient for the initial examination of experimental studies. However, further evaluation of the model with experiments is necessary due to measurement uncertainties in the mentioned studies. Third, we have proposed a straightforward optimization method using MATLAB's fsolve function (trust-region-dogleg algorithm) to find the optimal gas inflow rate. This approach demonstrated that by considering the physical implications of the system, it is possible to achieve the optimal point more efficiently. Finally, we have revealed that reservoir pressure significantly influences

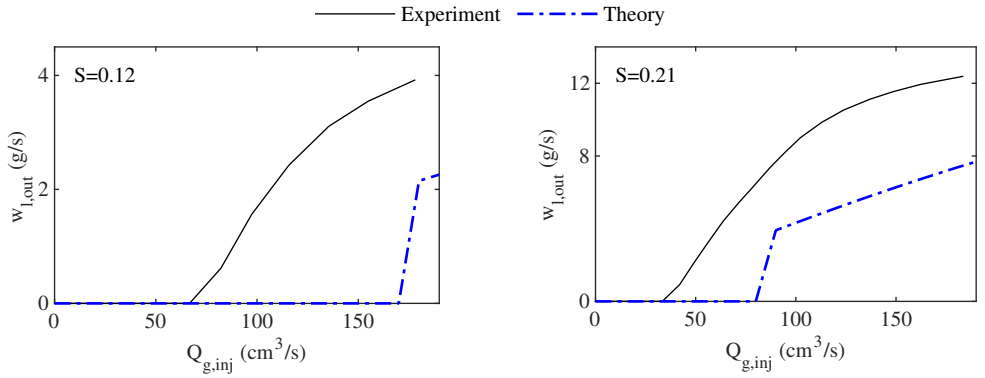

Figure 8: Comparing the mathematical model with experimental data from Becaria et al. (2006) [46]. S is the submergence ratio. The pipe diameter and height are 1.2 cm and 300 cm, respectively.

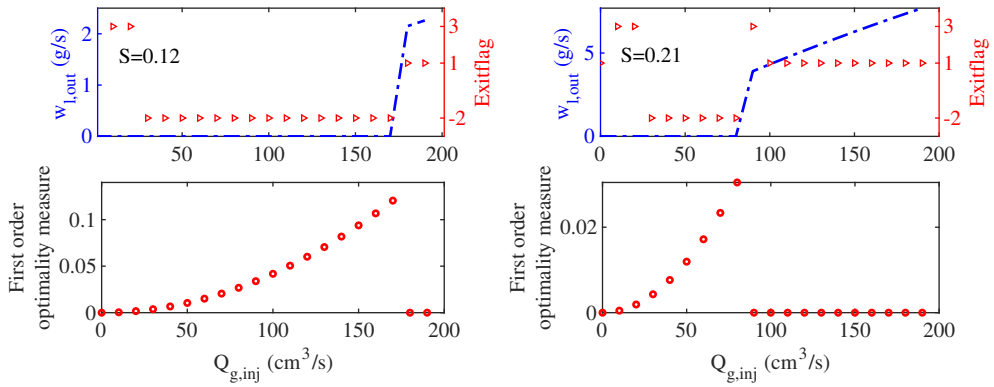

Figure 9: Solution quality of the proposed mathematical model for the study of Becaria et al. (2006) [46]. S is the submergence ratio. The pipe diameter and height are 1.2 cm and 300 cm, respectively.

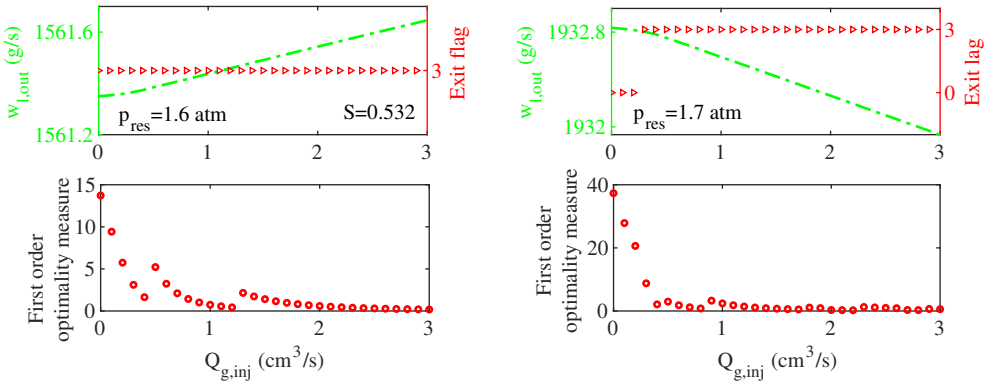

Figure 10: The proposed mathematical model for the study of Stenning and Martin (1968) [44]. S is the submergence ratio. The pipe diameter and height are 2.54 cm and 426.72 cm, respectively.

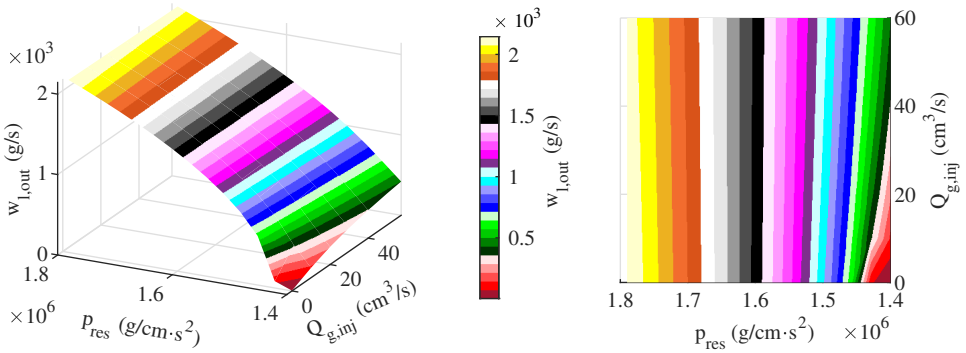

Figure 11: The proposed mathematical model for the study of Stenning and Martin (1968) [44]. The submergence ratio is 0.442. The pipe diameter and height are 2.54 cm and 426.72 cm, respectively.

Table 3: Evaluation metrics for theoretical results compared to experimental results.

S [44]	0.442	0.532	0.629	0.709		
MAE (%)	4.6	7.8	3.1	1.8		
RMSE (%)	5.4	9.3	3.5	2.3		
S [7]	0.227	0.300	0.484	0.570	0.670	0.750
MAE (%)	21.2	19.0	3.3	4.5	20.9	12.0
RMSE (%)	32.6	20.3	8	7.8	34.1	24.1
S [38]†	0.580	0.740				
MAE (%)	5.0	8.0				
RMSE (%)	8.7	8.8				
S [45]	0.400	0.500	0.600	0.700		
MAE (%)	27.1	16.6	20.2	24.0		
RMSE (%)	30.0	18.5	24.8	28.3		

S denotes the submergence ratio, MAE is the mean absolute error, and RMSE shows the root mean squared error.
† The metrics for the modified theory, see Eq. (31).
Stenning and Martin (1968) [44], Kassab et al. (2009) [7], Goharzadeh and Fernandes (2014 [38], Todoroki et al. (1973) [45].

the effectiveness of gas lift systems. Namely, reservoir pressure can determine whether the gas lift will increase or decrease the liquid outflow rate. For future investigations, researchers can apply the tailored version of this model to industrial applications. Furthermore, examining the impact of high and low liquid volume fractions on the fluid outflow rate could provide a clearer understanding of the relationship between liquid volume fraction and fluid outflow rate.

Acknowledgments

The Research Council of Norway, major international oil companies, and subsea system suppliers partially funded this research through the Research Innovation Center for Subsea Production and Processing (SUBPRO).

Declaration of generative AI and AI-assisted technologies in the writing process

During the preparation of this work the corresponding author used Grammarly AI prompts to improve the readibility of this article. After using this tool, the authors reviewed and edited the content as needed and takes full responsibility for the content of the published article.

References

[1] A. Hernandez, S. Gasbarri, M. Machado, L. Marcano, R. Manzanilla, J. Guevara, Field-scale research on intermittent gas lift, in: SPE Mid-Continent Operations Symposium, Oklahoma City, Oklahoma, USA, 1999, pp. SPE–52124–MS.
URL https://doi.org/10.2118/52124-MS

[2] O. Carlson, S. N. Bordalo, Experimental study of the dynamics and stability of intermittent gas-lift in a laboratory scale model, in: SPE Latin America and Caribbean Mature Fields Symposium, Salvador, Bahia, Brazil, 2017, pp. SPE–184919–MS.
URL https://doi.org/10.2118/184919-MS

[3] D. D. Croce, L. E. Zerpa, Effect of surface tension on sweeping performance of injected gas during intermittent gas lift in liquid loaded horizontal wells, in: SPE Annual Technical Conference and Exhibition, Virtual, 2020, pp. SPE–201601–MS.
URL https://doi.org/10.2118/201601-MS

[4] M. Descamps, R. V. A. Oliemans, G. Ooms, R. F. Mudde, R. Kusters, Influence of gas injection on phase inversion in an oil-water flow through a vertical tube, Int. J. Multiphas. Flow 32 (2006) 311–322.
URL https://doi.org/10.1016/j.ijmultiphaseflow.2005.10.006

[5] M. N. Descamps, R. V. A. Oliemans, R. F. Mudde, G. Ooms, Three-phase gas lift in the laboratory: air bubble injection into oil-water vertical pipe flow, in: 13th International Conference on Multiphase Production Technology, Edinburgh, the UK, 2007, pp. 253–261.
URL https://onepetro.org/BHRICMPT/proceedings-pdf/BHR07/All-BHR07/BHR-2007-D1/1801348/bhr-2007-d1.pdf

[6] M. N. Descamps, R. V. A. Oliemans, G. Ooms, R. F. Mudde, Experimental investigation of three-phase flow in a vertical pipe: local characteristics of the gas phase for gas-lift conditions, Int. J. Multiphas. Flow 33 (2007) 1205–1221.
URL https://doi.org/10.1016/j.ijmultiphaseflow.2007.06.001

[7] S. Z. Kassab, H. A. Kandil, H. A. Warda, W. H. Ahmed, Air-lift pumps characteristics under two-phase flow conditions, Int. J. Heat Fluid Fl. 30 (2009) 88–98.
URL https://doi.org/10.1016/j.ijheatfluidflow.2008.09.002

[8] V. Banjara, E. Pereyra, C. Avila, C. Sarica, Critical review & comparison of severe slugging mitigation techniques, Geoenergy Science and Engineering 228 (2023) 212082.
URL https://doi.org/10.1016/j.geoen.2023.212082

[9] Z. Schmidt, D. R. Doty, K. Dutta-Roy, Severe slugging in offshore pipeline riser-pipe systems, Soc. Petrol. Eng. J. 25 (1985) 27–38.
URL https://doi.org/10.2118/12334-PA

[10] Y. Taitel, Stability of severe slugging, Int. J. Multiphas. Flow 12 (1986) 203–217.
URL https://doi.org/10.1016/0301-9322(86)90026-1

[11] J. Fabre, L. L. Peresson, J. Corteville, R. Odello, T. Bourgeois, Severe slugging in pipeline/riser systems, SPE Prod. Eng. 5 (1990) 299–305.
URL https://doi.org/10.2118/16846-PA

[12] B. F. M. Pots, I. G. Bromilow, M. J. W. F. Konijn, Severe slug flow in offshore flowline/riser systems, SPE Prod. Eng. 2 (1987) 319–324.
URL https://doi.org/10.2118/13723-PA

[13] F. E. Jansen, O. Shoham, Y. Taitel, The elimination of severe slugging—experiments and modeling, Int. J. Multiphas. Flow 22 (1996) 1055–1072.
URL https://doi.org/10.1016/0301-9322(96)00027-4

[14] B. J. Brasjen, J. Veltin, J. H. Hansen, Mitigation of terain-induced slugging using mixer devices, in: SPE Annual Technical Conference and Exhibition, Amsterdam, the Netherlands, 2014, pp. SPE–170946–MS.
URL https://doi.org/10.2118/170946-MS

[15] F. E. Jansen, O. Shoham, Methods for eliminating pipeline-riser flow instabilities, in: SPE Annual Western Regional Meeting, Long Beach, California, USA, 1994, pp. SPE–27867–MS.
URL https://doi.org/10.2118/27867-MS

[16] J. E. Seim, V. L. Van Beusekom, R. A. W. M. Henkes, O. J. Nydal, Experiments and modeling for the control of riser instabilities with gas lift, in: 15th International Conference on Multiphase Production Technology, Cannes, France, 2011, pp. 19–31.
URL https://onepetro.org/BHRICMPT/proceedings-pdf/BHR11/All-BHR11/BHR-2011-A2/1663545/bhr-2011-a2.pdf

[17] C. A. Larsen, H. A. Asheim, Experimental investigation of gas lift instability and dynamic regulation to control it, in: SPE Annual Caspian Technical Conference and Exhibition, Astana, Kazakhstan, 2014, pp. SPE–172271–MS.
URL https://doi.org/10.2118/172271-MS

[18] C. H. P. Ribeiro, S. C. Miyoshi, A. R. Secchi, A. Bhaya, Model predictive control with quality requirements on petroleum production platforms, J. Petrol. Sci. Eng. 137 (2016) 10–21.
URL https://doi.org/10.1016/j.petrol.2015.11.004

[19] D. Krishnamoorthy, K. Fjalestad, S. Skogestad, Optimal operation of oil and gas production using simple feedback control structures, Control Eng. Pract. 91 (2019) 104107.
URL https://doi.org/10.1016/j.conengprac.2019.104107

[20] R. Dirza, J. Matias, S. Skogestad, D. Krishnamoorthy, Experimental validation of distributed feedback-based real-time optimization in a gas-lifted oil well rig, Control Eng. Pract. 126 (2022) 105253.
URL https://doi.org/10.1016/j.conengprac.2022.105253

[21] J. Matias, J. P. C. Oliveira, G. A. C. Le Roux, J. Jäschke, Steady-state real-time optimization using transient measurements on an experimental rig, J. Process Contr. 115 (2022) 181–196.
URL https://doi.org/10.1016/j.jprocont.2022.04.015

[22] S. Guet, G. Ooms, Fluid mechanical aspects of the gas-lift technique, Annu. Rev. Fluid Mech. 38 (2006) 225–249.
URL https://doi.org/10.1146/annurev.fluid.38.061505.093942

[23] H. T. Rodrigues, A. R. Almeida, D. C. Barrionuevo, R. S. Fraga, Effect of the gas injection angle and configuration in the efficiency of gas lift, J. Petrol. Sci. Eng. 198 (2021) 108126.
URL https://doi.org/10.1016/j.petrol.2020.108126

[24] L. A. O. Guerra, B. O. Temer, J. B. R. Loureiro, A. P. Silva Freire, Experimental study of gas-lift systems with inclined gas jets, J. Petrol. Sci. Eng. 216 (2022) 110749.
URL https://doi.org/10.1016/j.petrol.2022.110749

[25] G. O. Eikrem, O. M. Aamo, B. A. Foss, Stabilization of gas-distribution instability in single-point dual gas lift wells, SPE Production and Operations 21 (2006) 252–259.
URL https://doi.org/10.2118/97731-PA

[26] O. M. Aamo, G. O. Eikrem, H. B. Siahaan, B. A. Foss, Observer de-

sign for multiphase flow in vertical pipes with gas-lift—theory and experiments, J. Process Contr. 15 (2005) 247–257.
URL https://doi.org/10.1016/j.jprocont.2004.07.002

[27] G. O. Eikrem, O. M. Aamo, B. A. Foss, On instability in gas lift wells and schemes for stabilization by automatic control, SPE Production and Operations 23 (2008) 268–279.
URL https://doi.org/10.2118/101502-PA

[28] J. Zuo, W. Tian, S. Qiu, G. Su, Transient safety analysis for simplified accelerator-driven system with gas-lift pump, Prog. Nucl. Energ. 106 (2018) 181–194.
URL https://doi.org/10.1016/j.pnucene.2018.01.003

[29] J. Zuo, W. Tian, R. Chen, S. Qiu, G. Su, Research on enhancement of natural circulation capability in lead-bismuth alloy cooled reactor by using gas-lift pump, Nucl. Eng. Des. 263 (2013) 1–9.
URL https://doi.org/10.1016/j.nucengdes.2013.04.005

[30] M. Eriksson, Accelerator-driven systems: safety and kinetics, Doctoral dissertation, Royal Institute of Technology, Stockholm, Sweden (2005).
URL https://api.semanticscholar.org/CorpusID:108218169

[31] J.-P. Revol, An accelerator-driven system for the destruction of nuclear waste, Prog. Nucl. Energ. 38 (2001) 153–166.
URL https://doi.org/10.1016/S0149-1970(00)00100-1

[32] R. P. Coutinho, W. C. Williams, P. J. Waltrich, P. Mehdizadeh, S. Scott, J. Xu, W. Mabry, The case for liquid-assisted gas lift unloading, SPE Production and Operations 33 (2018) 73–84.
URL https://doi.org/10.2118/187943-PA

[33] D. Qi, H. Zou, T. Chen, Y. Ding, A method for comparison of lifting effects of plunger lift and continuous gas lift, J. Petrol. Sci. Eng. 190 (2020) 107101.
URL https://doi.org/10.1016/j.petrol.2020.107101

[34] NIST reference on constants, units, and uncertainty, https://physics.nist.gov/cuu/Constants/index.html, accessed 19 March 2024.

[35] NIST chemistry webbook, https://webbook.nist.gov/chemistry/fluid/, accessed 19 March 2024.

[36] G. O. Eikrem, O. M. Aamo, H. Siahaan, B. Foss, Anti-slug control of gas-lift wells—experimental results, in: 6th IFAC Symposium on Nonlinear Control Systems, Stuttgart, Germany, 2004, pp. 799–804.
URL https://doi.org/10.1016/S1474-6670(17)31323-X

[37] W. H. Ahmed, H. M. Badr, Dual-injection airlift pumps: an enhanced performance, Particul. Sci. Technol. 30 (2012) 497–516.
URL https://doi.org/10.1080/02726351.2011.604396

[38] A. Goharzadeh, K. Fernandes, Experimental characterization of a modified airlift pump, in: International Mechanical Engineering Congress and Exposition, Montreal, Quebec, Canada, 2014, pp. IMECE2014–39899.
URL https://doi.org/10.1115/IMECE2014-39899

[39] A. Oueslati, A. Megriche, The effect of liquid temperature on the performance of an airlift pump, Enrgy. Proced. 119 (2017) 693–701.
URL https://doi.org/10.1016/j.egypro.2017.07.096

[40] Z. Wang, Y. Kang, X. Wang, D. Li, D. Hu, Investigating the flow characteristics of air-lift pumps operating in gas-liquid two-phase flow, Chinese J. Chem. Eng. 26 (2018) 219–227.
URL https://doi.org/10.1016/j.cjche.2017.09.011

[41] Y. Liu, C. Yao, Development of an efficient numerical model for two-phase flows in air-lift pumps and its application to deep-sea mining, Ocean Eng. 281 (2023) 114897.
URL https://doi.org/10.1016/j.oceaneng.2023.114897

[42] F. C. Diehl, T. K. Anzai, C. S. Almeida, O. F. Von Meien, S. S. Neto, V. R. Rosa, M. C. M. M. Campos, F. Reolon, G. Gerevini, C. Ranzan, M. Farenzena, J. O. Trierweiler, Fast offshore wells model (FOWM): a practical dynamic model for multiphase oil production systems in deepwater and ultra-deepwater scenarios, Comput. Chem. Eng. 99 (2017) 304–313.
URL https://doi.org/10.1016/j.compchemeng.2017.01.036

[43] O. Egeland, J. T. Gravdahl, Hydraulic motors, 2nd Edition, Marine Cybernetics, 2003, Ch. 4, pp. 141–142.
URL https://folk.ntnu.no/oe/Modeling%20and%20Simulation.pdf

[44] A. H. Stenning, C. B. Martin, An analytical and experimental study of air-lift pump performance, J. Eng. Gas Turbines Power 90 (1968) 106–110.
URL https://doi.org/10.1115/1.3609143

[45] I. Todoroki, Y. Sato, T. Honda, Performance of air-lift pump, Bulletin of JSME 16 (1973) 733–741.
URL https://doi.org/10.1299/jsme1958.16.733

[46] J. Becaria, P. R. Toma, E. Kuru, Small-diameter gas lift systems—a potential technical solution for transport of fluids from low-pressure reservoirs, J. Can. Petrol. Technol. 45 (2006) 47–54.
URL https://doi.org/10.2118/06-06-03

[47] J. H. Spurk, N. Aksel, Fluid mechanics, 2nd Edition, Springer, Heidelberg, Germany, 2008, Ch. 9, pp. 279–284.
URL https://doi.org/10.1007/978-3-540-73537-3

[48] J. R. Blann, J. D. Williams, Determining the most profitable gas injection pressure for a gas lift installation, J. Petrol. Technol. 36 (1984) 1305–1311.
URL https://doi.org/10.2118/12202-PA